Direct measurements of strain depth profiles in Ge/Si(001) nanostructures

D. W. Moon and H. I. Lee
Nano Surface Group, Korea Research Institute of Standards and Science (KRISS), Doryong-dong 1, Taejon 305-606, Korea

B. Cho, Y. L. Foo,[a] T. Spila,[b] S. Hong,[c] and J. E. Greene
Department of Materials Science and the Frederick Seitz Materials Research Laboratory, University of Illinois, 104 South Goodwin Avenue, Urbana, Illinois 61801

(Received 18 August 2003; accepted 27 October 2003)

Direct measurements of strain depth profiles in Ge layers consisting of either pyramidal or dome-shaped nanostructures grown on Si(001) by gas-source molecular-beam epitaxy were obtained using medium-energy ion scattering spectroscopy. Layers consisting solely of pyramidal Ge structures (corresponding to total Ge coverages $\theta_{Ge}=5.5$ ML) exhibit a compressive strain of 2.1% which is uniform with depth. In contrast, Ge layers with a dome-shaped surface morphology ($\theta_{Ge}=8.9$ ML) undergo significant relaxation giving rise to a strain gradient which varies from 0.6% at the surface to 2.1% at the Ge/Si(001) interface. © *2003 American Institute of Physics.* [DOI: 10.1063/1.1635074]

Intensive effort has been devoted to understanding the growth and relaxation of strained Ge layers on Si(001). Ge/Si(001), with a 4.2% lattice mismatch, serves as a model system for the study of strain-driven roughening via the Stranski–Krastanow growth mode in which the initial formation of smooth two-dimensional (2D) wetting layers is followed by nucleation of three-dimensional (3D) islands with increasing layer thickness.[1–3] This mechanism of island formation provides a method for the self-assembled patterning of semiconductor nanostructures which have potential applications in device architectures.[4,5] Due to the effect of strain on electronic and optical properties, a detailed knowledge of the strain field associated with islands of varying size and shape is essential to the effective design and fabrication of devices incorporating strained nanostructures.[6]

Average strain values in thin Ge/Si(001) layers have been determined using ion scattering,[7] optical measurements of wafer curvature,[8] two-beam transmission electron microscopy (TEM) dark field imaging,[9] and x-ray diffraction (XRD).[6] Both wafer curvature and TEM results show a discontinuous change in strain accompanying the pyramid-to-dome transformation. XRD results suggest that Ge pyramids are highly strained near the interface, but relax progressively towards the apex of the pyramids. In each of these experimental techniques, however, the extraction of depth dependent information requires assumptions on the strain distribution in the islands. While numerical calculations of strain distributions in equilibrium island shapes have been carried out,[2,10] there have been no direct measurements.

In this letter, we report the results of experiments using medium-energy ion scattering spectroscopy (MEIS) to directly measure strain depth profiles in Ge wetting layers and two different types of Ge/Si(001) nanostructures: one consisting of only Ge pyramids, and one composed almost exclusively of Ge domes. MEIS provides both compositional and structural information with atomic layer depth resolution through analyses of energy and angular distributions of elastically scattered protons.[11,12] The strain depth profiles we obtain clearly show that Ge layers consisting entirely of pyramids exhibit a uniform in-plane compressive strain $\varepsilon_{\parallel}$ of 2.1%, while dome-dominated Ge/Si(001) surface morphologies exhibit a large gradient in $\varepsilon_{\parallel}$ ranging from 0.6% at the outer surface to 2.1% at the Ge/Si(001) interface.

All Ge layers were grown in a multichamber ultrahigh vacuum (UHV) gas-source molecular-beam epitaxy (GS-MBE) system[13,14] using Ge_2H_6.[15] The growth chamber, equipped with reflection high energy electron diffraction (RHEED), is connected through a transfer chamber to an analytical station which includes Auger electron spectroscopy (AES). Precursor gases are delivered to the substrate through individual tubular dosers located 3 cm from the substrate at an angle of 45°. The dosers are coupled to feedback-controlled constant-pressure reservoirs in which pressures are separately monitored using capacitance manometers whose signals are used to regulate variable leak valves. Valve sequencing, pressures, gas flows, and film growth temperatures are all computer controlled.

Substrates used in these experiments are *n*-type Si(001) wafers with a miscut of 0.2° toward [110]. Following substrate cleaning,[16] degassing at 600 °C in UHV for >4 h, and flash heating to 1100 °C, we grow a 50-nm-Si buffer layer at 800 °C using Si_2H_6. This provides a clean atomically flat Si(001) starting surface exhibiting sharp 2×1 RHEED patterns with no contamination detectable by AES. Ge(001) wetting layers and ultrathin films whose surfaces consist of pyramidal nanostructures were grown at a temperature T_s of 500 °C with an incident Ge_2H_6 flux $J_{Ge_2H_6}$ of 2.8×10^{15} cm^{-2} s^{-1} while layers consisting of dome-shaped nanostructures were grown at $T_s=600$ °C with $J_{Ge_2H_6}=5.2\times10^{15}$ cm^{-2} s^{-1}. The Ge deposition rates were 32.4 and

[a]Institute of Materials Research and Engineering (IMRE), 3 Research Link, S(117602), Singapore.
[b]Author to whom correspondence should be addressed; electronic mail: tspila@uiuc.edu
[c]School of Materials Science and Engineering, Seoul National University, San 56-1, Shilim-dong, Kwanak-ku, Seoul 151-744, Korea.

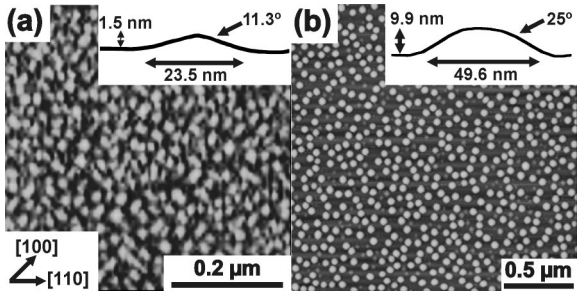

FIG. 1. AFM images of (a) pyramidal-shaped Ge nanostructures in a 5.5-ML-thick layer grown at 500 °C on Si(001) and (b) domed-shaped nanostructures in an 8.9-ML-thick Ge layer grown at 600 °C. Typical line profiles are shown in the insets.

47.1 ML min^{-1}, respectively. Ge coverages θ_{Ge} were determined by Rutherford backscattering spectrometry (RBS) while tapping-mode atomic force microscopy (AFM) was used to image surface morphologies. Samples for which strain profiles were determined by MEIS were capped *in-situ* with a 3-nm-thick amorphous Si layer, deposited by electron-beam evaporation, prior to air exposure.

MEIS strain depth profile measurements were carried out using a 100 keV incident H^+ beam aligned 4° from the [001] direction in the (011) plane of the Si(001) substrate. We measure the angular distribution of protons scattered $\pm 10°$ around the $[11\bar{1}]$ direction in the (011) plane. Shifts in $[11\bar{1}]$ Ge blocking dips are obtained as a function of depth with the bulk Si substrate $[11\bar{1}]$ blocking dip serving as the reference position.

Typical AFM images, with line profiles in the insets, are shown in Fig. 1 for each of the two types of Ge nanostructure samples. AFM images from Ge wetting layers ($\theta_{Ge} \leqslant 3$ ML) grown under the same deposition conditions as used to obtain Ge pyramids, exhibit no morphological contrast indicating that the layers are very flat, with rms roughnesses $\leqslant 0.22$ nm, as expected. Figure 1(a) corresponds to a $\theta_{Ge} = 5.5$ ML sample consisting of only square-based pyramid-shaped islands, with sides along ⟨100⟩ directions, which cover approximately 42% of the surface area. The average pyramid size ℓ is 17.7 ± 3.5 nm with a height $h = 1.5 \pm 0.3$ nm and a sidewall angle $\varphi = 11.3°$ corresponding to {105} facets. Figure 1(b) is an AFM image of a Ge layer with $\theta_{Ge} = 8.9$ ML grown at 600 °C. The surface is composed of uniformly-sized domes with $\ell = 48.7 \pm 2.9$ nm and $h = 10.1 \pm 0.8$ nm. The domes, which cover 35% of the surface area, are highly faceted. When viewed along a ⟨110⟩ zone axis, as in the inset of Fig. 1(b), the dominant facet has a sidewall angle of $\sim 25°$ corresponding to {113}, in agreement with previous AFM and low energy electron microscopy observations of Ge/Si(001) domes.[17,18] Based upon the total number of Ge atoms measured by RBS and the total mound volume determined from AFM, the thickness of the Ge wetting layer between the mounds is $\leqslant 0.5$ nm.

Figure 2 is a typical series of $[11\bar{1}]$ MEIS blocking dips plotted as a function of sample depth, in this case for the sample with dome-shaped islands shown in Fig. 1(b). Each successive blocking dip represents an additional 300 eV energy loss corresponding to 1 nm in layer thickness. Nearly all of the Ge signal derives from the mound structures since the wetting layer between the mounds is $\leqslant 0.5$ nm. The Si(001) substrate blocking dip is also shown for reference. Note that the positions of the blocking dips obtained from Ge near the Ge/Si(001) interface are shifted to higher scattering angles with respect to that of the bulk Si(001) substrate clearly demonstrating that the bottom of the dome-shaped Ge islands are compressively strained. However, the strain relaxes toward the surface as indicated by the fact that the Ge blocking dip moves toward the position of the bulk Si substrate blocking dip. We also note that Si near the film/substrate interface between the mounds is compressively strained in agreement with theoretical predictions in Ref. 19 and may also indicate Ge/Si intermixing as expected for Ge/Si(001) growth at 600 °C.[20]

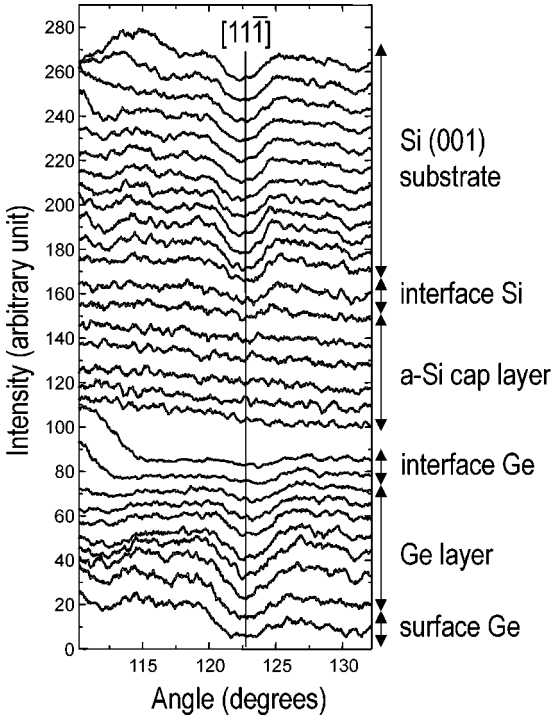

FIG. 2. MEIS $[11\bar{1}]$ blocking dips as a function of depth through the Ge layer with dome-shaped islands corresponding to Fig. 1(b) above.

Shifts in Ge blocking dip minima, as well as local tetragonal distortions, obtained from Fig. 2 are plotted as a function of depth in Fig. 3. Based upon similar MEIS measure-

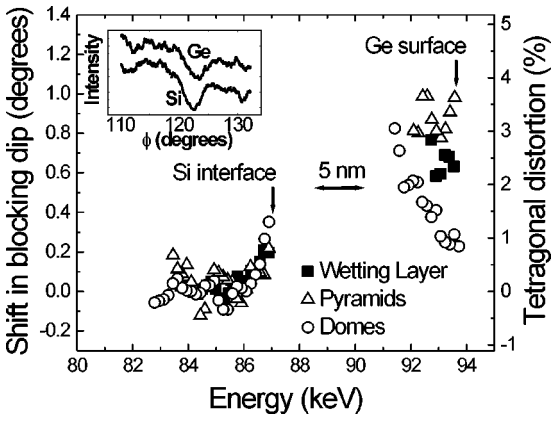

FIG. 3. Shifts in MEIS blocking dips and strain depth profiles through Ge/Si(001) layers whose surfaces consist of Ge wetting layers, Ge pyramids, and Ge domes. Typical Ge and Si blocking dips for pyramid structures and the bulk Si substrate are shown in the inset.

ments, strain depth profiles for a Ge wetting layer grown at $T_s = 500\,^{\circ}\mathrm{C}$ and a sample consisting of Ge pyramids are also shown. Absolute minimum positions were determined by fitting the blocking dips with a quadratic function. The 1.8-ML-thick wetting layer has a uniform in-plane compressive strain of $\varepsilon_{\parallel} = 1.6 \pm 0.4\%$. Samples with a surface morphology consisting solely of {105} faceted pyramids are also in compression with a tetragonal distortion of 3.3% which is constant to within $\pm 0.4\%$ as a function of depth. Using the Ge Poisson ratio of 0.277,[6] $\varepsilon_{\parallel}$ in the pyramids is 2.1%. In contrast, the strain profile of the dome-dominated structure is strongly depth dependent and exhibits an approximately linear decrease in $\varepsilon_{\parallel}$ from 2.1% near the substrate to 0.6% at the surface. Our MEIS results are consistent with analytic continuum model calculations[2,10,19] showing nearly uniform strain depth profiles in surface islands having small aspect ratios near the size of our pyramids and significant strain gradients, similar to that shown in Fig. 3, in larger islands near the size of our domes. The calculations also reveal that substrate compliance is important and can relax up to approximately 40% of the island strain depending upon aspect ratio.

In conclusion, we have used MEIS measurements to directly measure strain depth profiles of Ge islands on Si(001). We observe significant changes in the strain profile as the islands transform from pyramidal to dome-shaped with increasing Ge layer thickness. 5.5-ML-thick Ge layers whose surfaces are composed of square pyramids with an average size of 17.7-nm and an aspect ratio of 0.08, exhibit a uniform compressive strain of 2.1%. Samples with $\theta_{\mathrm{Ge}} = 8.9$ ML and grown under conditions such that the surface structure is essentially all rounded domes with an average size of 48.7 nm and an aspect ratio of 0.21 also have a compressive strain of 2.1% at the film/substrate interface, but the strain decreases approximately linearly to 0.6% at the surface. Thus, strain relaxation is intimately related to the pyramid-to-dome island shape transformation.

The authors acknowledge the financial support of MOST, Korea through the National Research Laboratory program and the Atomic Scale Surface Science Research Center, U.S. Department of Energy, Division of Materials Sciences, under Contract DEFG02-ER9645439 and NSF Division of Materials Research Grant DMR 97-05440. We are also grateful for the use of the facilities in the Center for Microanalysis of Materials, which is partially supported by the DOE, at the University of Illinois.

[1] D. J. Eaglesham and M. Cerullo, Phys. Rev. Lett. **64**, 1943 (1990).
[2] B. J. Spencer and J. Tersoff, Phys. Rev. Lett. **79**, 4858 (1997).
[3] F. M. Ross, R. M. Tromp, and M. C. Reuter, Science **286**, 1931 (1999).
[4] R. F. Service, Science **271**, 920 (1996).
[5] G. Abstreiter, P. Schittenhelm, C. Engel, E. Silveira, A. Zrenner, D. Marteens, and W. Jager, Semicond. Sci. Technol. **11**, 1521 (1996).
[6] A. J. Steinfort, P. M. L. O. Scholte, A. Ettema, F. Tuinstra, M. Nielsen, E. Landemark, D.-M. Smilgies, R. Feidenhans'l, G. Falkenberg, and R. L. Johnson, Phys. Rev. Lett. **77**, 2009 (1996).
[7] A. T. Fiory, J. C. Bean, L. C. Feldman, and I. K. Robinson, J. Appl. Phys. **56**, 1227 (1984).
[8] J. A. Floro, E. Chason, L. B. Freund, R. D. Twesten, R. Q. Hwang, and G. A. Lucadarno, Phys. Rev. B **59**, 1990 (1999).
[9] C.-P. Liu, J. M. Gibson, D. G. Cahill, T. I. Kamins, D. P. Basile, and R. S. Williams, Phys. Rev. Lett. **84**, 1958 (2000).
[10] B. J. Spencer and J. Tersoff, Phys. Rev. B **63**, 205424 (2000).
[11] J. F. van der Veen, Surf. Sci. Rep. **5**, 199 (1985).
[12] S.-J. Kahng, Y. H. Ha, J.-Y. Park, S. Kim, D. W. Moon, and Y. Kuk, Phys. Rev. Lett. **80**, 4931 (1998).
[13] D. Lubben, R. Tsu, T. R. Bramblett, and J. E. Greene, J. Vac. Sci. Technol. A **9**, 3003 (1991).
[14] T. R. Bramblett, Q. Lu, T. Karasawa, M.-A. Hasan, S. K. Jo, and J. E. Greene, J. Appl. Phys. **76**, 1884 (1994).
[15] A. Vailionis, B. Cho, G. Glass, P. Desjardins, D. G. Cahill, and J. E. Greene, Phys. Rev. Lett. **85**, 3672 (2000).
[16] H. Kim and J. E. Greene, J. Vac. Sci. Technol. A **17**, 354 (1999).
[17] F. M. Ross, R. M. Tromp, and M. C. Reuter, Science **286**, 1931 (1999).
[18] S. A. Chaparoo, Y. Zhang, J. Drucker, D. Chandrasaekar, and D. J. Smith, J. Appl. Phys. **87**, 2245 (2000).
[19] R. V. Kukta and L. B. Freund, J. Mech. Phys. Solids **45**, 1835 (1997).
[20] K. Nakajima, A. Konishi, and K. Kimura, Phys. Rev. Lett. **83**, 1802 (1999).